VOL. 15, NO. 20, OCTOBER 2020 ISSN 1819-6608
ARPN Journal of Engineering and Applied Sciences

www.arpnjournals.com

DEVELOPMENT A LOW-COST NAVIGATION TECHNOLOGY BASED ON METAL LINE SENSORS AND PASSIVE RFID TAGS FOR INDUSTRIAL AUTOMATED GUIDED VEHICLE

V. Rubanov, D. Bushuev, E. Karikov, A. Bazhanov and S. Alekseevsky
Department of Technical Cybernetics, BSTU N.A. V.G. Shukhov, Russia
E-Mail: vgrubanov@gmail.com

ABSTRACT

The choice of type and structure of the automatically self-driven vehicle and used navigation technology is essential when developing the automatic warehouse systems. Common navigation technologies often used in large warehouse systems such as Amazon or Alibaba are expensive enough for use in small and medium-sized enterprises. This paper describes the process of developing a low-cost navigation technology for automatically guided vehicles based on industrial inductive sensors detecting metalized lines and RFID localization. This work presents the AGV structure and the basic algorithms for motion control and navigation. Virtual and physical AGV models are presented, as well as test results with similar control system parameters.

Keywords: automated guided vehicle, navigation, RFID, metal line sensor, virtual prototype, fault tolerance.

1. INTRODUCTION

Automated guided vehicles normally mean mobile self-driven robots used in transporting objects [1]. They are widely used in warehouse systems and flexible automated lines of large enterprises and retailers. At the same time, the main reason for limiting the introduction of industrial self-driven vehicles in small and medium-sized enterprises is their high cost and, accordingly, a long payback period.

One of the ways to cost-reducing of AGV is to simplify the principles of navigation, localization and positioning while maintaining operational reliability and the possibility of flexible generation and change of driving routes.

There are new technologies for mobile robot navigation actively developed now. A low-cost solution is to build systems for indoor navigation based on Wi-Fi [2] and Bluetooth beacon [3] technologies. The positioning accuracy with this method of navigation is low that makes it difficult to create an industrial AGV based on it. A promising direction is the application of an approach combining simultaneous localization and mapping (SLAM) with the implementation of machine vision systems, laser or ultrasound scanners of ambient space of mobile robots [4-7]. However, the AGV group control is implemented more simply and reliably, if there are certain motion instructions: the motion route, marks, etc. Therefore, in warehouse complexes and flexible manufacturing AGV navigation systems are still mainly implemented using the following sensor technologies [8,9]: inductive wire and magnetic line following guidance, color line guidance, laser guidance, magnetic spots guidance, barcode guidance. The disadvantage of methods using laser and optical technologies is the high pollution sensitivity, which limits the application at some industrial enterprises. In general, industrial implementations of the previously noted navigation systems are quite expensive.

In [10] it was proposed to use a metal line and three discrete inductive sensors to set the motion path of a mobile robot. Information about the state of inductive sensors is used to determine the motion direction of the differential drive. This method of the line following driving is insensitive to pollution and, in addition, allows to reduce the cost of laying the route in comparison with magnetic or conductive lines. However, in the presence of intersections and branches, this method is not applicable for navigation and, in addition, in the presence of wheel slip the system goes into a self-oscillating mode of motion from the left to the right sensor.

In the papers [11-14] it is proposed to use a grid of radio frequency identification tags (RFID) located on the floor covering composed for navigation. To create a grid when implementing this method requires a sufficiently large number of passive RFID tags.

In the present paper, there is proposed a complex AGV navigation technology combining motion along a metalized line with proportional-differential control of lateral deviation and coding of turns and technological sections (charging, loading, unloading) using RFID tags. This approach will create a low-cost AGV navigation system based on industrial inductive sensors and a small number of passive RFID tags and thereby reduce the cost of implementing an automated warehouse or flexible production.

Before manufacturing a physical AGV prototype, in order to verify the proposed navigation technology, it is necessary to conduct a series of virtual tests [15]. Manufacturers of AGV and their components usually offer simulation software, for example, RoboAGVSim, Flexsim, Anylogic, Simcad. Such software is designed to explore how AGV works with known navigation technologies. There are also universal modeling tools in the field of robotics: GAZEBO, SimTwo, MORSE or Unity3D [15]. The process of developing AGV models with new types of sensor systems using these tools is quite time-consuming.

In our case, a more flexible solution was required, which allows further research of the AGV dynamics in the case of defects in mechanical components and failures of control system elements. For this purpose, there was built a virtual AGV prototype with elements of the warehouse system in the MSC Adams software, it was integrated into the warehouse motion control system implemented in the Matlab/Simulink software. This made it possible to conduct joint dynamics modeling of AGV motion control systems inside the virtual warehouse space under various modes. After conducting virtual tests, a physical prototype was implemented and tested. The results of the tests confirmed the efficiency of the proposed technology.

This paper has the following organization: Sect. 2 describes the proposed navigation technology, digital model and hardware implementation of the AGV prototype; Sect. 3 presents the results and Sect. 4 shows the conclusions.

2. METHODOLOGY

2.1 Proposed Navigation Technology

Figure-1 shows the structure of AGV with a differential drive that implements the proposed navigation technology. This mobile robot has two driven hub motors with brushless DC motors (BLDC) and three caster wheels. The rotation speed of each hub motors is set by the BLDC controllers CU1-CU2.

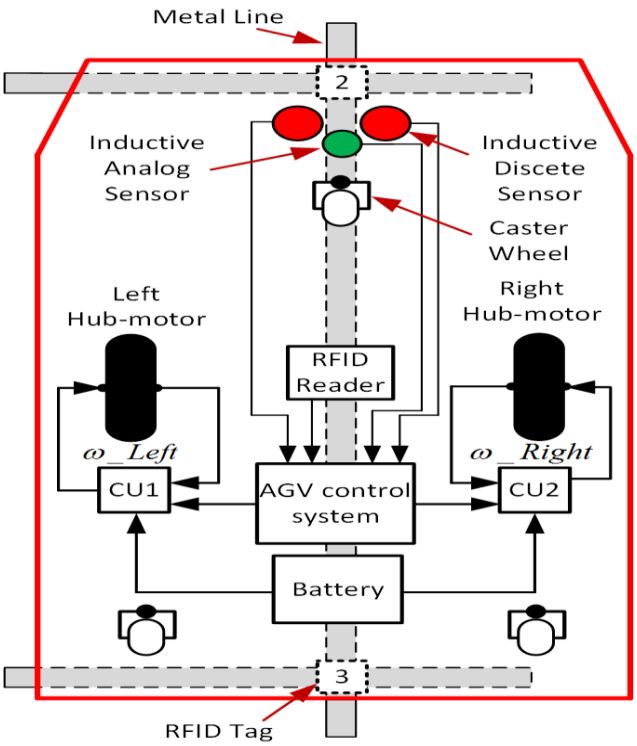

Figure-1. Mobile platform structure.

The RFID reader antenna connected to the corresponding processing board is located at the center of the platform. An analog inductive sensor in the AGV center and two discrete DP sensors are used as metalized line sensors and placed so that their outputs are in a low state while moving without lateral deviation. Inductive sensors use eddy current principle. Therefore, the AGV motion path can be set using a standard thin metalized tape glued to the floor. Passive RFID tags are used to navigate at the intersection of the route lines, as well as at the points of start and stop. The current point number and numbers of its neighbors are recorded in the RFID memory in the predefined order. For the *i*-th tag, such a vector has the following form [i, left, front, right, behind]. If there is no tag on either side, then the corresponding element is 0. An example of a route section is shown in Figure-2.

The motion controller sets ω_Left_S and ω_Right_S for the speed controllers of the hub motors.

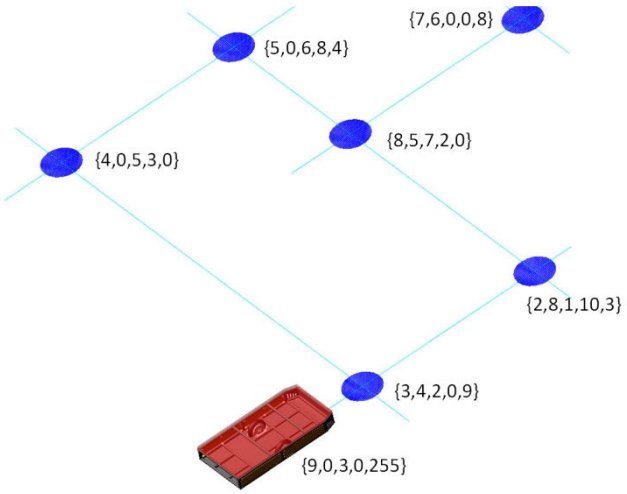

Figure-2. Warehouse tracks implementation.

During the line following mode automatic compensation of lateral deviation is carried out using information from three inductive sensors. The presence of a central analog sensor generating the signal $e(t)$ allows implementing a discrete P- or PD law to control lateral deviation by changing the rotation speed of the right ω_{Right} or left ω_{Left} hub motor in accordance with algorithm 1. In this case, the side discrete sensors are used to determine the direction of change error $e(t)$. Here, ω_{Ref} is the rotation speed of the right and left hub motors when moving in a straight line, k_p is the gain, T_d is the derivative action time, T_0 is the sampling time.

The algorithm also takes into account the deadband of inductive sensors while moving above the RFID tag.

The line following mode is activated until the RFID tag is detected. After reading the RFID tag, a further decision on the choice of the motion direction is made on the basis of the recorded tag information and the number of the next target RFID tag according to the AGV route based on the algorithm 2.

The turn end condition is triggered corresponding discrete sensors: for the left turn - the left sensor, and for the right - the right one. Then the line following mode is switched on again till the next RFID tag.

2.2 Co-Simulation Model of the AGV and Warehouse Tracks

Figure-3 presents the structure of the proposed navigation technology for simulation the dynamics of AGV movement. The mechanical model part of the transport system section contains a virtual AGV prototype, the wheels of which are connected through Solid-to-Solid contacts with the floor covering. Warehouse tracks are defined as polylines, at the intersection of which there are RFID tags located (see. Figure-2). When exporting a control plant using the Adams.Controls module, a cmd file is generated to build the model in the Adams. View software tool. Matlab supports the automatic selection of the RFID tags location points and their neighbors, as well as the lines of warehouse tracks, from this file. Then an oriented graph is generated, which is the base for searching the shortest route of AGV motion. At the output of the Path Planning subroutine we have a Route array containing a sequence of RFID tags that have to be passed through the endpoint reaching.

Algorithm 1 Lateral Deviation Control

procedure DEVIATIONCONTROL
  if LeftSensor && RightSensor **then**
    $\omega_{Right} \leftarrow \omega_{Ref}$
    $\omega_{Left} \leftarrow \omega_{Ref}$
  else
    if $\Delta > \epsilon$ **then**
      if LeftSensor **then** $\omega_{Right} \leftarrow \omega_{Ref} + k_p T_d \epsilon[k] + T_d (\epsilon[k] - \epsilon[k-1]) / T_0$
      if RightSensor **then** $\omega_{Left} \leftarrow \omega_{Ref} + k_p T_d \epsilon[k] + T_d (\epsilon[k] - \epsilon[k-1]) / T_0$
  return ω_{Right}, ω_{Left}

Algorithm 2 Path-following algorithm

procedure PATHMOTION(prev_tag,route)
prev_tag – last reached tag
route = $[n, r_0, r_1, \ldots, r_n]$ array with path points (RFID tags), where n – count of points, r_i – point number
  this_target ← 1
  this_tag ← 0
  environment ← [0, 0, 0, 0] ▷ array with nearest tags
  status ← *operating_state*
  while *status* == *operating_state* **do**
    if *new tag found* **then**
      (*this_tag*, *environment*) ← *ReadTag*() ▷ read current and nearest tag
      if (*this_tag* == *route*[*route*[0]]) **then**
        status ← *ok* ▷ reaching final point
        route ← [0] ▷ ready for new task
      else
        if then(*this_tag* == *route*[*this_target*])
          this_target + +
          while (*prev_tag*! = *environment*[0]) **do**
            environment << 1 ▷ cyclic shift
          if (*route*[*this_target*] == *environment*[1]) **then**
            stop and turn left
          if (*route*[*this_target*] == *environment*[2]) **then**
            straight forward moving
          if (*route*[*this_target*] == *environment*[3]) **then**
            stop and turn right
          prev_tag ← *this_tag*
  return (*status*, *prev_tag*)

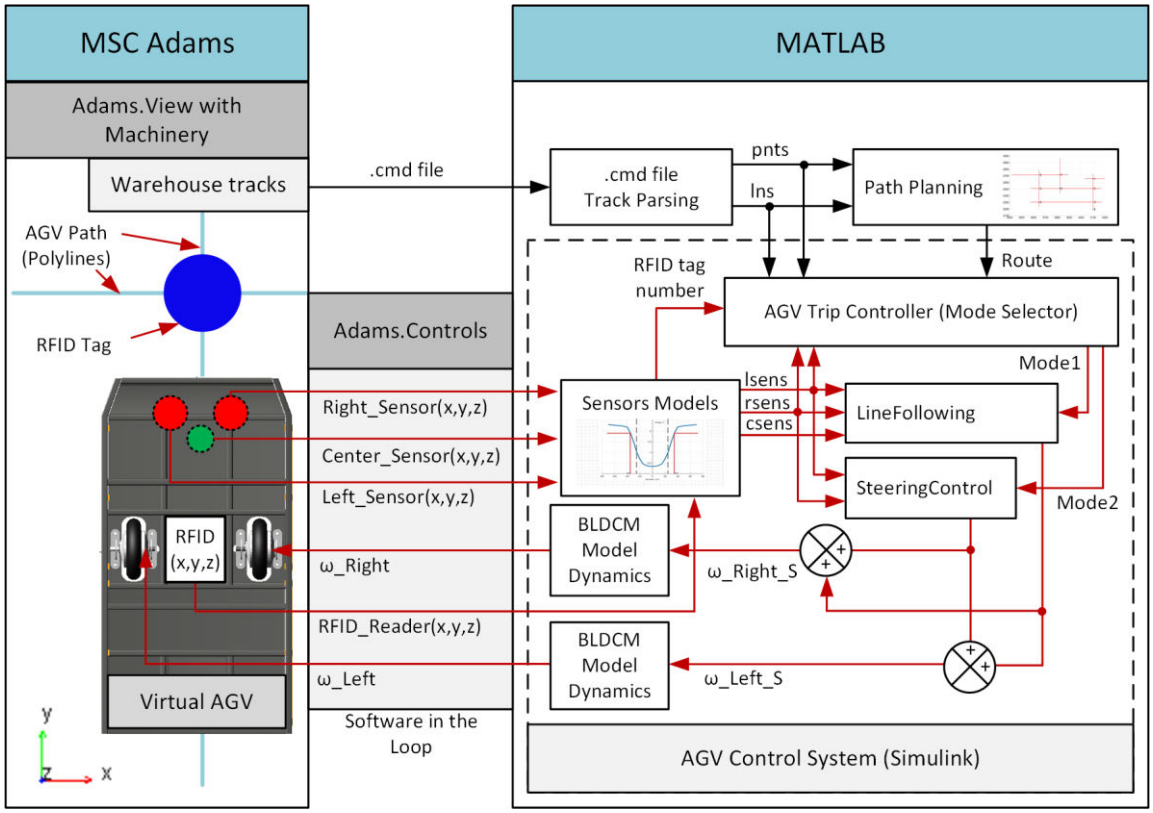

Figure-3. AGV Co-simulation model structure.

The simulation of the sensor subsystem is as follows. The distance to the shortest metalized line is determined for each inductive sensor in accordance with algorithm 3 using the coordinates (*x*,*y*,*z*) of the inductive sensors coming from the Adams Control Plant to the Sensors Models subroutine in the Matlab/Simulink software. Then logical signal levels *lsens* and *rsens* for discrete inductive sensors are formed in accordance with the experimentally determined response range.

Algorithm 3 DistanceLinePoint

procedure DISTANCELINEPOINT(pnts,lns,pnt)
pnts – array of $n \times 3$ elements with graph vertices coordinates
lns – array of $m \times 2$ elements with graph edges coordinates, where coordiantes are graph vertices indexes in pnts
pnt – coordinates (x,y,z) of the point to which the distance is measured
  $dist \leftarrow zeros(m, 1)$
  for $i \leftarrow 1 : m$ **do**
    $p0 \leftarrow pnts(lns(i, 1), :)$
    $p1 \leftarrow pnts(lns(i, 2), :)$ ▷ $p0$ и $p1$ vertex of line with i index
    $dx \leftarrow p1(1) - p0(1)$ ▷ Difference between coordinates X
    $dy \leftarrow p1(2) - p0(2)$ ▷ Difference between coordinates Z
    $dz \leftarrow p1(3) - p0(3)$ ▷ Difference between coordinates Y
    $tmin \leftarrow \left([dx\ dy\ dz]^T \cdot (pnt - p0)\right) / \left(dx^2 + dy^2 + dz^2\right)$
    if $tmin \leq 0$ **then**
      $dist \leftarrow \sqrt{sum((pnt - p0). * (pnt - p0))}$
    else if $tmin > 0$ *and* $tmin < 1$ **then**
      $p_{near} \leftarrow p0 + tmin * [dxdydz]$
      $dist \leftarrow \sqrt{sum((pnt - p_{near}). * (pnt - p_{near}))}$
    else
      $dist \leftarrow \sqrt{sum((pnt - p1). * (pnt - p1))}$
  return *dist*

The transition to the *csens* voltage signal for an analog inductive sensor is carried out using interpolation (for example, using the LookUpTable function) and the experimentally obtained nonlinear unimodal static map.

The nearest tag (from the *pnts* array) is continuously searched on the basis of the RFID reader coordinates and if they fall into the coverage area of the simulated readers, then information tag is read from the tag taking into account delays associated with the periods of polling and data transfer via interfaces in the processing board.

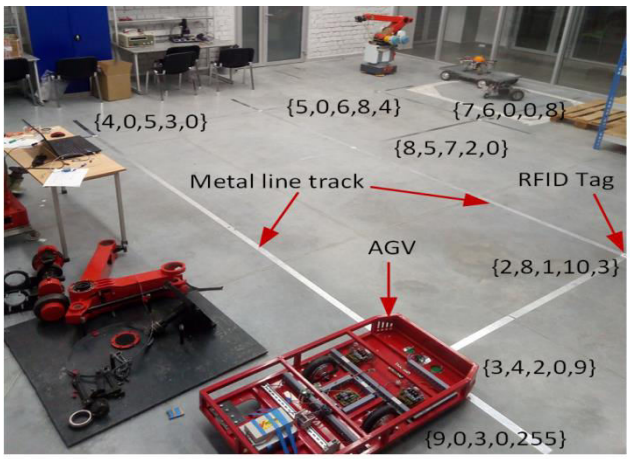

Figure-4. The experimental test setup.

The AGV Trip Controller selects the AGV Line Following or Steering Control mode depending on the route, the found RFID tags and the logic states of the discrete inductive sensors.

The settings for the hub motor speed controllers *ω_Left_S* and *ω_Right_S* are formed in the line following and turning mode with carrying out using algorithms 1 and 2, the "LineFollowing" and "SteeringControl" subroutines, respectively. A virtual prototype [16], reproducing the processes in a brushless DC motor and the mechanical part of the planetary mechanism could be used to describe the hub motor dynamics. However, in the presented structure a dynamic model is used to accelerate the calculation, it is specified by approximating the mathematical model of real hub motors with a first-order relaxation circuit with delay. The delay is due to the conversion of information from Hall sensors using the M-method [17], as well as the sampling time.

2.3 Hardware Implementation Of The Experimental Test Setup

The proposed navigation technology and AGV were implemented in accordance with the developed virtual prototype. The sensor subsystem uses the DPA-F60-40U-2110-N analog inductive sensor, VBI-F80-40S-2113-Z discrete sensors, and the RFID tag reader MicroEm UEM Mifare ICode NFC reader v6. The RFID tag reader has a sampling frequency of 20 Hz (50 ms) and 50 ms is spent on sending through the RS-485 interface to the AGV control system, thus, the transport delay value is $\tau = 100$ ms, which limits the maximum speed of the AGV. The metalized tape has a 50 mm width, at which the output of the analog sensor goes into saturation with a lateral deviation of more than 4 cm, and discrete sensors have a response radius of 40 mm. Thus, the sensing areas of the discrete and analog sensors intersect.

Hub motor CU1-CU2 and AGV controllers are based on the STM32F103C8T6 microcontroller. Green-E-Motion hub motors with a speed control system are described by the transfer function $W_{HM}(s) = e^{-0.13s}/(0.05\ s + 1)$, where s is the Laplace operator.

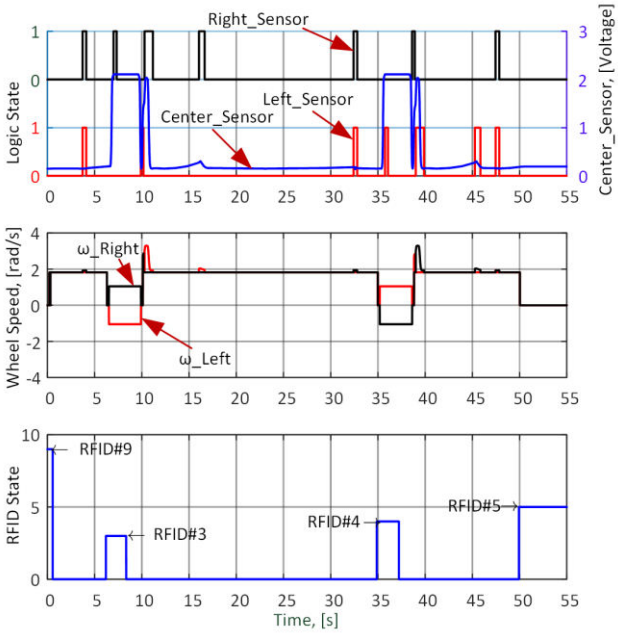

Figure-5. Results of AGV dynamics modeling.

3. RESULTS

Virtual and pilot tests were conducted for testing the operability of the proposed navigation technology. Figure-5 and Figure-6 show the dynamics of the virtual prototype and physical prototype on the route [9,3,4,5] (See Figure-2 and Figure-4). The rotation speed of hub motors without lateral deviation in a straight motion $\omega_{Ref} = 1.8$ rad / s, and in the rotation mode $\omega_{Ref} = 1$ rad / s. Taking into account the radius of the motor wheel $R = 0.1$ m, the AGV motion speed $V \approx 0.20$ m / s.

In general, the results of computer simulation and pilot testing at the test site are consistent. The rotation time of the prototype corresponds to computer simulation, and the time of its general motion is almost 5 s longer than during model tests due to more frequent compensation of lateral deviation. The total distance traveled by the motor wheels is defined as:

$$S = \frac{R}{T_0}\int_0^T \omega(t)dt$$

For experimental tests $S_R = 8.3$ m, the total traveled distance was approximately one meter longer than in virtual tests for which $S_V = 7.3$ m. This is due to uneven floors and the presence of non-linearities that were not taken into account in the simulation.

4 CONCLUSIONS

According to the modeling results and experimental tests, the proposed navigation technology has confirmed its operability. The developed virtual prototype with a control system practically corresponds to the physical one and can be expanded to test group control algorithms, diagnose failures of onboard control systems and restore its functioning. As future work can be considered usage of two analog inductive sensors that generate a differential signal, which will reduce the effect of the floor covering unevenness, a thickness change of the metalized line. As a result, the lateral deviation will decrease.

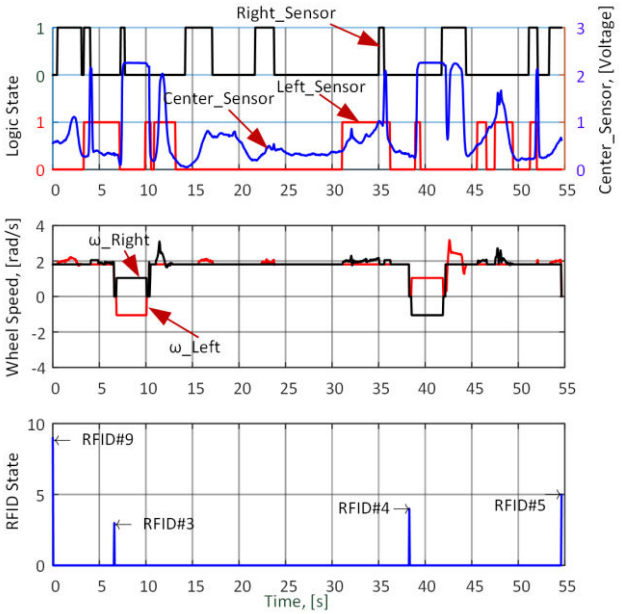

Figure-6. Results of the motion control system work of the physical prototype.

ACKNOWLEDGEMENTS

Research is carried out with the financial support of The Ministry of Science and Higher Education of the Russian Federation within the Public contract project 2.1396.2017/4.6.

REFERENCES

[1] Li Q., Adriaansen A.C., Udding J.T., Pogromsky A.Y. 2011. Design and Control of Automated Guided Vehicle Systems: A Case Study. IFAC Proceedings Volumes. 44(1): 13852-13857.

[2] Biswas J., Veloso V. 2010. WiFi Localization and Navigation for Autonomous Indoor Mobile Robot. International Conference on Robotics and Automation: 4379-4384.

[3] Mackey A., Spachos P., Plataniotis K.N. 2018. Enhanced Indoor Navigation System with Beacons and Kalman Filters. IEEE Global Conference on Signal and Information Processing (GlobalSIP): 947-950.

[4] Borenstein J., Everett H.R., Feng L., Wehe D. 1997. Mobile Robot Positioning - Sensors and Techniques. Journal of Robotic Systems. 14(4): 231-249.

[5] Labbe M., Michaud F. 2014. Online global loop closure detection for large-scale multi-session graph-based SLAM. IEEE/RSJ International Conference on Intelligent Robots and Systems: 2661-2666.

[6] Labbe M., Michaud F. 2017. Long-term online multi-session graph-based SPLAM with memory management. Autonomous Robots. 42: 1133-1150.

[7] Fedorko G., Honus S., Salai R. 2017. Comparison of the Traditional and Autonomous AGV Systems. MATEC Web of Conferences. 134.

[8] Lynch L., Newe T., Cliford J., Coleman J., Walsh J. 2018. Automated Ground Vehicle (AGV) and Sensor Technologies - A Review. 12th International Conference on Sensing Technology (ICST). 347-352.

[9] Lee S.-Y., Yang H.-W. 2012. Navigation of automated guided vehicles using magnet spot guidance method. Robotics and Computer-Integrated Manufacturing. 28(3): 425-436.

[10] Rashid M.Z.A., Shah H.N.M., Aras M.S.M., Kamaruddin M.N., Kassim A.M., Jaaafar H.I. 2014. Metal Line Detection: A New Sensory System for Line Following Mobile Robot. Journal of Theoretical and Applied Information Technology. 64(3): 756-764.

[11] Hubacz M., Pawlowicz B., Trybus B. 2019. Using Multiple RFID Readers in Mobile Robots for Surface Exploration. Conference on Automation. 920: 445-456.

[12] Park S., Hashimoto S. 2009. Autonomous Mobile Robot Navigation Using Passive RFID in Indoor Environment. IEEE Transactions on Industrial Electronics. 56(7): 2366-2373.

[13] Park S., Hashimoto S. 2010. Autonomous Navigation System for Mobile Robot Using Randomly Distributed Passive RFID Tags. IEICE Transactions on Fundamentals of Electronics, Communications and Computer Sciences. 93-A(4): 711-719.

[14] Han S., Lim H.-S., Lee J.-M. 2017. An Efficient Localization Scheme for a Differential-Driving

Mobile Robot Based on RFID System. IEEE Transactions on Industrial Electronics. 54(6): 3362-3369.

[15] Allmacher C., Klimant P., Chemnitz TU. 2019. Test Course Creation for Automated Guided Vehicles. Simulation in Produktion und Logistik (2019) // ASIM SPL 2019 At: Chemnitz, Germany.: Matthias Putz & Andreas Schlegel (Hrsg.) Wissenschaftliche Scripten, Auerbach.

[16] Bushuev D.A., Kiseleva T.Y., Rubanov V.G. 2019. Virtual prototype for co-simulation of hub-motor dynamics with brushless DC motor and elements of fault-tolerant control. IOP Conf. Series: Materials Science and Engineering. 560.

[17] Kim S. H. Electric Motor Control DC, AC, and BLDC Motors Elsevier. 2017. Chapter 9. Speed estimation and sensorless control of alternating current motors: 373-388.